High-resolution study of Gamow-Teller excitations in the ^{42}Ca(^{3}He,t) ^{42}Sc reaction and the observation of a "low-energy super-Gamow-Teller state"

Y. Fujita,[1,2,*] H. Fujita,[1,2] T. Adachi,[1] G. Susoy,[1,3] A. Algora,[4,5] C. L. Bai,[6] G. Colò,[7] M. Csatlós,[5] J. M. Deaven,[8,9,10] E. Estevez-Aguado,[4] C. J. Guess,[8,9,10,†] J. Gulyás,[5] K. Hatanaka,[1] K. Hirota,[1] M. Honma,[11] D. Ishikawa,[1] A. Krasznahorkay,[5] H. Matsubara,[1,‡] R. Meharchand,[8,9,10,§] F. Molina,[4,‖] H. Nakada,[12] H. Okamura,[1,¶] H. J. Ong,[1] T. Otsuka,[13] G. Perdikakis,[8,14] B. Rubio,[4] H. Sagawa,[15,16] P. Sarriguren,[17] C. Scholl,[18,#] Y. Shimbara,[19] E. J. Stephenson,[20] T. Suzuki,[1] A. Tamii,[1] J. H. Thies,[21] K. Yoshida,[22] R. G. T. Zegers,[8,9,10] and J. Zenihiro[1,**]

[1]*Research Center for Nuclear Physics, Osaka University, Ibaraki, Osaka 567-0047, Japan*
[2]*Department of Physics, Osaka University, Toyonaka, Osaka 560-0043, Japan*
[3]*Department of Physics, Istanbul University, Istanbul 34134, Turkey*
[4]*Instituto de Física Corpuscular, CSIC-Universidad de Valencia, E-46071 Valencia, Spain*
[5]*Institute of Nuclear Research (ATOMKI), H-4001 Debrecen, Post Office Box 51, Hungary*
[6]*Department of Physics, Sichuan University, Chengdu 610065, China*
[7]*Dipartimento di Fisica, Università degli Studi di Milano, via Celoria 16, 20133 Milan, Italy*
[8]*National Superconducting Cyclotron Laboratory, Michigan State University, East Lansing, Michigan 48824-1321, USA*
[9]*Joint Institute for Nuclear Astrophysics, Michigan State University, East Lansing, Michigan 48824, USA*
[10]*Department of Physics and Astronomy, Michigan State University, East Lansing, Michigan 48824, USA*
[11]*Center for Mathematical Science, University of Aizu, Aizu-Wakamatsu, Fukushima 965-8580, Japan*
[12]*Department of Physics, Chiba University, Inage, Chiba 263-8522, Japan*
[13]*Department of Physics, University of Tokyo, Hongo, Bunkyo, Tokyo 113-0033, Japan*
[14]*Department of Physics, Central Michigan University, Mount Pleasant, Michigan 48859, USA*
[15]*Center for Mathematics and Physics, University of Aizu, Aizu-Wakamatsu, Fukushima 965-8580, Japan*
[16]*RIKEN, Nishina Center, Wako Saitama 351-0198, Japan*
[17]*Instituto de Estructura de la Materia, IEM-CSIC, Serrano 123, E-28006 Madrid, Spain*
[18]*Institut für Kernphysik, Universität zu Köln, 50937 Köln, Germany*
[19]*CYRIC, Tohoku University, Aramaki, Aoba, Sendai 980-8578, Japan*
[20]*Center for Exploration of Energy and Matter, Indiana University, Bloomington, Indiana 47408, USA*
[21]*Institut für Kernphysik, Westfälische Wilhelms-Universität, D-48149 Münster, Germany*
[22]*Graduate School of Science and Technology, Niigata University, Niigata 950-0913, Japan*

(Received 14 January 2015; revised manuscript received 20 May 2015; published 26 June 2015)

To study the Gamow-Teller (GT) transitions from the $T_z = +1$ nucleus ^{42}Ca to the $T_z = 0$ nucleus ^{42}Sc, where T_z is the z component of isospin T, we performed a (p,n)-type (^{3}He ,t) charge-exchange reaction at 140 MeV/nucleon and scattering angles around 0°. With an energy resolution of 29 keV, states excited by GT transitions (GT states) could be studied accurately. The reduced GT transition strengths B(GT) were derived up to the excitation energy of 13 MeV, assuming the proportionality between the cross sections at 0° and B(GT) values. The main part of the observed GT transition strength is concentrated in the lowest 0.611-MeV, $J^\pi = 1^+$ GT state. All the other states at higher energies are weakly excited. Shell-model calculations could reproduce the gross feature of the experimental B(GT) distribution, and random-phase-approximation calculations including an attractive isoscalar interaction showed that the 0.611-MeV state has a collective nature. It was found that this state has all of the properties of a "low-energy super-Gamow-Teller state." It is expected that low-lying $J^\pi = 1^+$ GT states have $T = 0$ in the $T_z = 0$ nucleus ^{42}Sc. However, $T = 1$ states are situated in a higher energy region. Assuming an isospin-analogous structure in $A = 42$ isobars, analogous $T = 1$, 1^+ states are also expected in ^{42}Ca. Comparing the ^{42}Ca(^{3}He ,t) ^{42}Sc and ^{42}Ca(p,p') spectra measured at 0°, candidates for $T = 1$ GT states could be found in the 10–12-MeV region of ^{42}Sc. They were all weakly excited. The mass dependence of the GT strength distributions in Sc isotopes is also discussed.

DOI: 10.1103/PhysRevC.91.064316 PACS number(s): 21.10.Hw, 25.55.Kr, 27.40.+z, 25.40.Ep

*fujita@rcnp.osaka-u.ac.jp
†Present address: Department of Physics and Astronomy, Swarthmore College, Swarthmore, Pennsylvania 19081, USA.
‡Present address: NIRS, Inage, Chiba 263-8555, Japan.
§Present address: Institute for Defense Analyses, Alexandria, Virginia 22206, USA.
‖Present address: Comisión Chilena de Energía Nuclear, Post Office Box 188-D, Santiago, Chile.
¶Deceased.
#Present address: Institute for Work Design of North Rhine-Westphalia, Radiation Protection Services, 40225 Düsseldorf, Germany.
**Present address: RIKEN Nishina Center, Wako, Saitama 351-0198, Japan.

I. INTRODUCTION

Gamow-Teller (GT) transitions are mediated by the $\sigma\tau$ operator. Therefore, they are characterized as isovector (IV)-type spin-flip transitions with no angular momentum transfer ($\Delta \boldsymbol{T} = \mathbf{1}$, $\Delta \boldsymbol{S} = \mathbf{1}$, and $\Delta \boldsymbol{L} = 0$). The transitions are among the $j_>$ and $j_<$ shells such as $f_{7/2}$ and $f_{5/2}$ shells. Owing to the simple character of the GT operator, GT transitions are important tools for the study of nuclear structure [1–4] as well as nuclear interactions [5–8]. In addition, GT transitions are the most common nuclear weak-interaction processes. The GT strength functions in the pf-shell nuclei are important in estimating the rate of neutrino-induced reactions, β decays, and electron-capture processes for nucleosynthesis during the late stage of stellar evolution [9].

Gamow-Teller transitions are studied through β decays and charge-exchange (CE) reactions [4]. Studies using β decay can provide the most direct information on the reduced GT transition strength B(GT). However, the accessible energy region is limited by the decay Q value. In CE reactions, on the other hand, GT excitations can be studied up to high excitation energies. In particular, GT excitations become prominent at intermediate incident energies (above 100 MeV/nucleon) and forward angles around 0° [4,10]. Since the 1980s, (p,n) reactions performed at incoming proton energies of $E_p =$ 120–200 MeV have been used for the study of GT transitions in the β^- direction [10]. One of the most important findings was the structure named the Gamow-Teller resonance (GTR) situated at the high excitation energies of $E_x =$ 9–16 MeV. The GTRs, with bumplike structures having a width of a few MeV and carrying the main part of the observed GT transition strength, have been systematically studied in nuclei with mass number A larger than ≈50 [5,10,11].

In addition, in CE reactions performed at intermediate incident energies and 0°, it was found that there is a close proportionality between the GT cross sections and the B(GT) values [12,13],

$$\sigma^{\mathrm{GT}}(q,\omega) \simeq K(\omega) N_{\sigma\tau} |J_{\sigma\tau}(q)|^2 B(\mathrm{GT}) \quad (1)$$

$$= \hat{\sigma}^{\mathrm{GT}} F(q,\omega) B(\mathrm{GT}), \quad (2)$$

where $J_{\sigma\tau}(q)$ is the volume integral of the effective interaction $V_{\sigma\tau}$ at a momentum transfer q (≈0), $K(\omega)$ is the kinematic factor, ω is the total energy transfer, and $N_{\sigma\tau}$ is a distortion factor. The value $\hat{\sigma}^{\mathrm{GT}}$ is the unit cross section for the GT transition at $q = \omega = 0$ and a given incoming energy for a system with mass A. The value $F(q,\omega)$ gives the dependence of the GT cross sections on the momentum and energy transfers. It has a value of unity at $q = \omega = 0$ and usually decreases gradually as a function of excitation energy (E_x). It can be obtained from distorted-wave Born approximation (DWBA) calculations.

In (p,n)-type (^{3}He ,t) reactions, the close proportionality of Eq. (2) has been demonstrated to hold for $\Delta L = 0$ transitions with $B(\mathrm{GT}) \geqslant 0.04$ in studies of the mass $A =$ 23, 26, 27, and 34 sd-shell nuclear systems [14–18] and also for the mass $A =$ 46, 50, and 54 f-shell nuclei [19]. The deviations were a few to 10% (note that poorer agreement was also found in some specific cases; see the discussions in Ref. [4]). In these mass A systems, the strengths of multiple, analogous GT transitions with $T_z = \pm 1/2 \rightarrow \mp 1/2$ or $T_z = \pm 1 \rightarrow 0$ could be compared in the (^{3}He ,t) and β-decay studies. Here T_z is the z component of isospin T defined by $T_z = (N - Z)/2$, where N and Z are the proton (π) and neutron (ν) numbers, respectively.

The energy resolutions achieved in the pioneering (p,n) reactions were around 300 keV or greater. The advantage of using the (^{3}He ,t) reaction is that a higher-energy resolution can be achieved. At the Research Center for Nuclear Physics (RCNP), Osaka, excellent resolutions of ≈30 keV have been achieved at the ^{3}He beam energy of 140 MeV/nucleon. As a result, in the studies of GT excitations on $T_z = +1$ target nuclei ^{54}Fe [20] and ^{58}Ni [21] performed up to $E_x \approx 13$ MeV it was found that the bumplike structures of GTRs observed in (p,n) studies actually consist of many discrete states excited by GT transitions (GT states). The fragmented GT states were also observed in the studies of the other $T_z = +1$ target nuclei ^{46}Ti [22] and ^{50}Cr [23] and in a recent study of the $T_z = +3/2$ nucleus ^{47}Ti [24].

In a simple shell-model (SM) picture of the $T_z = +1$ nucleus ^{42}Ca, two neutrons in the $f_{7/2}$ shell are on top of the ^{40}Ca core, in which the sd shells are filled with protons and neutrons and an $N = Z = 20$ magic nucleus is formed. In this picture, two GT states excited by $\nu f_{7/2} \rightarrow \pi f_{7/2}$ and $\nu f_{7/2} \rightarrow \pi f_{5/2}$ transitions are expected in the low-lying region and the region about 5–6 MeV higher, respectively, where the 5–6 MeV is the energy difference of the $\pi f_{5/2}$ and $\pi f_{7/2}$ shells [1]. The GT excitations in ^{42}Sc were studied in a ^{42}Ca$(p,n)^{42}$Sc reaction at $E_p = 160$ MeV in the 1980s [25]. Contrary to the simple SM expectation, they found that the GT strength was mainly concentrated in the 0.61-MeV low-lying state and the strength in the higher E_x region was weak. Owing to the poor resolution of ≈800 keV, however, even the $T = 1$, $J^\pi = 0^+$ ground state (g.s.) [the isobaric analog state (IAS) of the g.s. of ^{42}Ca] and the first excited GT state at 0.61 MeV could not be separated. To study the Fermi and GT excitations having the $\Delta L = 0$ nature in detail, we performed a high-resolution (^{3}He ,t) reaction at very forward angles including 0°. The GT strength distribution up to $E_x \approx 13$ MeV is discussed.

II. EXPERIMENT

The ^{42}Ca(^{3}He ,t)^{42}Sc experiment was performed at the high-resolution facility of RCNP [26], consisting of the "WS course" beam line [27] and the "Grand Raiden" spectrometer [28] using a 140 MeV/nucleon ^{3}He beam from the $K = 400$ Ring Cyclotron [26]. The measurement was performed by setting the spectrometer at 0°. In the 0° measurement, both the ^{3}He^{2+} beam and the tritons enter the first dipole magnet (D1 magnet) of the spectrometer. The ^{3}He^{2+} beam with a magnetic rigidity $B\rho$ of about half that of the tritons was stopped in a Faraday cup placed inside the D1 magnet. The target was a self-supporting foil of enriched (93.7%) ^{42}Ca with an areal density of 1.78 mg/cm^2. The main contaminant isotope in the target was ^{40}Ca (5.1%).

The outgoing tritons were analyzed in momentum within the full acceptance of the spectrometer and detected with a focal-plane detector system that allowed for particle identification and track reconstruction in the horizontal and vertical

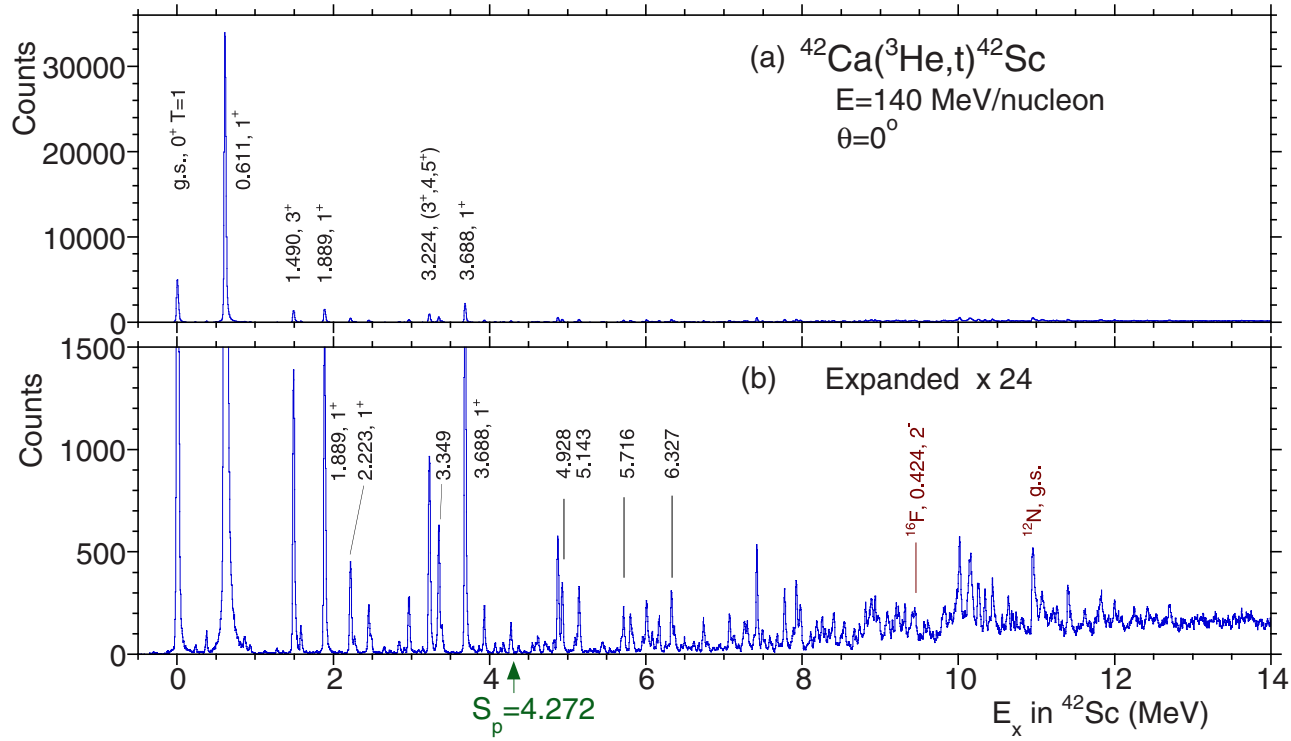

FIG. 1. (Color online) The 0°, ^{42}Ca(^{3}He,t)^{42}Sc spectrum on two scales. The events within the range of scattering angles $\Theta \leqslant 0.5°$ are included. (a) The full count range spectrum. Two prominent peaks are observed in the low-energy region and less prominent ones up to 4 MeV. (b) The vertical scale is magnified by a factor of 24. A fine structure of many states is observed up to $E_x = 12.7$ MeV. Major states populated in $\Delta L = 0$ transitions ($\Delta L = 0$ states) below 7 MeV are indicated by their excitation energies in MeV. The $\Delta L = 0$ states in the region above 7 MeV are indicated in Fig. 5(a) in Sec. IV.

directions [29]. Close to 0°, the scattering angle Θ can be expressed by $\sqrt{\theta^2 + \phi^2}$, where θ and ϕ are the scattering angles in the horizontal and vertical directions, respectively. An angular resolution $\Delta\Theta \leqslant 5$ mrad [full width at half maximum (FWHM)] was achieved by applying the *angular dispersion matching* technique [30] and the *overfocus mode* of the spectrometer [31]. In the analysis, the acceptance of the spectrometer, covering θ of $\pm 1°$ and ϕ of $\pm 2.5°$ was subdivided into five angular ranges (cuts) using the tracking information. Further experimental details are found in Refs. [20,21,32]. An energy resolution ΔE of 29 keV (FWHM), which is much better than the energy spread of $\approx$140 keV of the beam, was realized by applying the *lateral dispersion matching* and *focus matching* techniques [30,33].

The "0° spectrum" obtained for the events within the scattering angles $\Theta \leqslant 0.5°$ is shown in Fig. 1 up to $E_x = 13$ MeV. We measured the spectrum up to $E_x = 25$ MeV, but the spectrum was continuous and flat; no discrete peak was observed above 13 MeV. As we see from Fig. 1(a), there are only two strongly excited states. Referring to the evaluation given in Ref. [34], we could easily identify that they are the $T = 1$, $J^\pi = 0^+$ g.s. (i.e., the IAS) and the $T = 0$, $J^\pi = 1^+$, 0.611-MeV state. Most other states are weakly excited. In particular, states populated in transitions with $\Delta L \geqslant 1$, except the $J^\pi = 3^+$ state at 1.490 MeV, were weakly excited at 0°. We see that the (^{3}He,t) reaction at forward angles including 0° and at the incoming energy of 140 MeV/nucleon is well suited for the study of states populated in $\Delta L = 0$ transitions.

The gross feature of the 0° spectrum is in good agreement with that obtained in the ^{42}Ca(p,n)^{42}Sc reaction at $E_p =$ 160 MeV and 0° shown in Ref. [25]. As mentioned, they could not separate the g.s. and the first excited state at 0.61 MeV. With our $\approx$30 times better resolution, we see the fine structure of highly fragmented states. In a later (p,n) work [35], the g.s., i.e., the IAS, and the 0.61-MeV GT state were separated with a better resolution of $\Delta E \approx 300$ keV. However, they were interested in the study of the IAS and not in the GT excitations.

III. DATA ANALYSIS

The acceptance of the 0° setting of the spectrometer was subdivided into five angle cuts of $\Theta \leqslant 0.5°$, 0.5°–0.8°, 0.8°–1.2°, 1.2°–1.6°, and 1.6°–2.0°. The positions and intensities of peaks were obtained up to $E_x = 13$ MeV by applying a peak-decomposition program using the shape of the well-separated peak at 0.611 MeV as a reference.

Above the proton separation energy S_p of 4.27 MeV, a continuum caused by quasifree scattering (QFS) appears [36]. Accordingly, above $E_x \approx 5.5$ MeV, the continuous counts gradually increase with E_x [see Fig. 1(b) and also Fig. 5(a) in Sec. IV]. Therefore, a smooth empirical background connecting the deepest valleys between peaks was subtracted in the peak-decomposition analysis.

A. Excitation energy

As shown in Table I, only a few $J^\pi = 1^+$ states are known in ^{42}Sc [34]. Therefore, the E_x values of higher excited states

TABLE I. States in ^{42}Sc evaluated in Ref. [34] and observed in the ^{42}Ca(^{3}He,t)^{42}Sc reaction up to $E_x = 4.5$ MeV. The uncertainties for evaluated E_x values (the first column) are given in the cases where they are greater than 1 keV. Observed counts of states in the angle range $\Theta = 0^\circ$–0.5° are shown as "Counts (0°)." The B(GT) values are given for the states populated in $\Delta L = 0$ transitions.

Evaluated values[a]		(^{3}He,t)[b]			
E_x (MeV)	J^π	E_x (MeV)	ΔL	Counts (0°)	B(GT)
0.000	0^+, IAS	0.0	0	34 563(543)[c]	
0.611	1^+	0.612	0	241 037(1069)	2.173(47)[d]
1.490	3^+	1.491		10 039(156)	
1.586	2^+	1.586		666(46)	
1.846(2)	(3^+)				
1.874(8)	0^+				
1.889	1^+	1.887	0	10 701(159)	0.097(3)
2.188	$(2,3)^+$				
2.223	(1)	2.220	0	3081(110)[e]	0.028(1)
2.269	$(1,2^+)$	2.272		486(42)	
2.389	3^+				
2.455(2)	$(1,2^+)$	2.452	0	1537(73)	0.014(1)
2.487	2^+	2.484		460(53)	
2.833	$(2^+,3,4^+)$				
		2.841		457(35)	
2.848	3^+				
2.964		2.967	0	1946(69)	0.018(1)
3.224	$(3^+,4,5^+)$	3.229		6572(139)[e]	
3.345(4)		3.349	0	4418(112)	0.040(1)
3.393	$(1,2,3)^+$	3.389		521(64)[e]	
3.688	1^+	3.686	0	13 768(182)	0.127(3)
3.866(5)	1^+				
3.934	$(1,2,3)^+$	3.931		1499(62)	
4.067(10)		4.070		334(31)	
4.175(5)	$(3,4,5)^+$	4.177		333(34)	
4.276(5)		4.272		904(48)	
4.370(5)		4.370		245(27)	
4.548(5)	(2 to 5)$^+$	4.547		345(33)	

[a]From Ref. [34].
[b]Present work.
[c]Contribution of the counts from the IAS of ^{44}Sc and ^{43}Sc are subtracted.
[d]Calculated using the ^{42}Ti → ^{42}Sc β-decay data.
[e]Contribution of the count from ^{44}Sc is subtracted.

were determined from their peak positions in the $\Theta \leqslant 0.5^\circ$ spectrum with the help of kinematic calculations. As a reference, we used a (^{3}He,t) spectrum from a natural magnesium ($^{\rm nat}$Mg) target. The $^{\rm nat}$Mg target foil was thin (≈1.5 mg/cm^2) and the spectrum was taken under the same experimental conditions as for the ^{42}Ca target. The relationship between the peak positions in the spectrum and the corresponding values of magnetic rigidity of the spectrometer was determined using the well-known E_x values of states in ^{26}Al and ^{24}Al and the peak positions of these states.

The reaction Q values in the (^{3}He,t) reaction for the isotopes ^{26}Mg and ^{24}Mg are −4.0 and −13.9 MeV, respectively, and that of ^{42}Ca(^{3}He,t) is −6.4 MeV. The E_x values of ^{26}Al states up to 7.8 MeV are well known. The E_x values of a few low-lying states in ^{24}Al up to 1.09 MeV are also well known. The E_x values of higher excited states in ^{24}Al were determined in a recent β^+-decay study of ^{24}Si [37], although the uncertainties were larger (≈10 keV). Therefore, all E_x values of ^{42}Sc states up to $E_x = 11.8$ MeV listed in Tables I–IV were determined by interpolation.

We could reproduce most of the evaluated E_x values given in Ref. [34] up to 4.5 MeV within differences of ⩽4 keV, as seen in Table I. Because the g.s. excitation energy (i.e., $E_x = 0.0$ MeV) of ^{12}N from the ^{12}C contaminant seen at 10.95 MeV in the ^{42}Sc spectrum [see Fig. 1(b)] was reproduced with a deviation of less than 10 keV, we estimate that the uncertainty of E_x determination is approximately 10 keV even at $E_x = 11$ MeV. However, the level density became high above $E_x \approx 9$ MeV and many of the states can be multiplets. Therefore, in Tables III and IV, we list E_x values only for the isolated peaks with good statistics. In addition, we noticed that each state became wider above 11 MeV. Note that these high E_x states can have decay widths, because $S_p = 4.27$ MeV. For these states, the determination of the peak center became less accurate and we estimate an ≈±20 keV uncertainty in E_x values. Above 13 MeV, as mentioned, no sharp peak was observed.

B. Assignment of angular momentum transfer ΔL

It is expected that $J^\pi = 1^+$ states populated in $\Delta L = 0$ GT transitions have an angular distribution peaked at 0°. Figure 2 shows the angular distributions of well-separated $\Delta L = 0$ and $\Delta L \geqslant 1$ states observed in the low-E_x region. The vertical scale shows the counts of peaks (states) in the spectrum of $\Theta \leqslant 0.5^\circ$ cut and the counts in the larger angle cuts are normalized by the ratios of solid angles. We see that the 1^+ states at 0.611 and 1.889 MeV show almost identical decreasing pattern with the increase of scattering angle. We take the pattern of the 0.611-MeV state as the reference of the $\Delta L = 0$ angular distribution. However, $\Delta L \geqslant 1$ states show increasing patterns.

For the practical and quantitative identification of the decreasing "$\Delta L = 0$ pattern" of the angular distribution, we examined the "ratio of ratio" of counts in different angle cuts for each excited state. First, the peak counts of a state in the five angle cuts, i.e., $\Theta \leqslant 0.5^\circ$, 0.5°–0.8°, 0.8°–1.2°, 1.2°–1.6°, and 1.6°–2.0° cuts, were divided by the $\Theta \leqslant 0.5^\circ$ peak count of the state itself (naturally the ratio is one for the $\Theta \leqslant 0.5^\circ$ cut). Then these five ratios for each state were further divided by the corresponding ratios of the most prominent $J^\pi = 1^+$, 0.611-MeV state representing the decreasing $\Delta L = 0$ pattern (again the value of this ratio of ratio is one for the $\Theta \leqslant 0.5^\circ$ cut in each state). As a result, it is expected that a state having the $\Delta L = 0$ angular distribution should have the ratio of ratio of approximately 1 also in the four larger angle cuts. However, the ratio of ratio of a $\Delta L \geqslant 1$ state increases in larger angle cuts. Keeping the differences of the $\Delta L = 0$ and $\Delta L \geqslant 1$ angular distributions in mind (see Fig. 2), the $\Delta L = 0$ assignment was given if a state shows the ratio of ratio of 0.8–1.2 in all four larger angle cuts (for practical examples, see Refs. [36,38]).

The results of the $\Delta L = 0$ assignments for the peaks (states) clearly observed in the 0° spectrum [i.e., states with an intensity corresponding to a B(GT) value larger than ≈0.004]

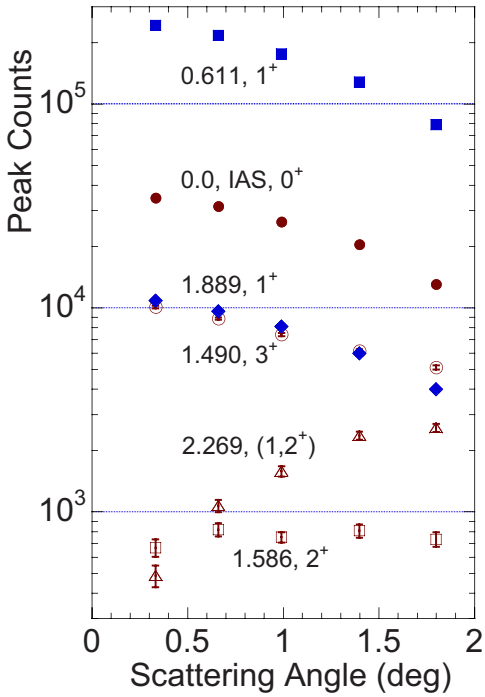

FIG. 2. (Color online) Angular distributions of $\Delta L = 0$ and $\Delta L \geqslant 1$ states observed in the low-E_x region of the (^{3}He,t) measurements. The E_x values and J^π values are from Ref. [34]. The vertical scale shows the counts of individual states in the spectrum of the $\Theta \leqslant 0.5^\circ$ cut. They are shown as "Counts (0°)" in Table I. The counts in the spectra with larger angle cuts are corrected by the ratios of the solid angles.

are indicated by the label "0" in Tables I–IV. These $\Delta L = 0$ states are indicated by their excitation energies in Figs. 1(a) and 1(b) and also in Fig. 5(a) shown in Sec. IV. In the higher E_x region, the level density is higher and many of the states are weakly excited. Therefore, $\Delta L = 0$ assignments are less certain for these states. They are indicated by the label "(0)" in Tables II–IV.

Most of the states given the assignments of higher J values in Ref. [34] (see column 2 of Table I) were assigned to have a $\Delta L \geqslant 1$ character by the larger ratios in larger angle cuts. However, two low-lying states at 1.490 and 3.224 MeV with the (possible) assignment of $J^\pi = 3^+$ [34] showed similar behavior to the 1^+ states in the smaller angle cuts of 0.5°–0.8° and 0.8°–1.2°. Larger ratios were observed only in the 1.2°–1.6° and 1.6°–2.0° cuts (the ratio of ratio was larger by ≈30% in the 1.6°–2.0° cut; see also Fig. 2). Therefore, the ratios in these higher angle cuts were examined with a care.

The g.s. of ^{42}Sc is the IAS of the g.s. of ^{42}Ca [34]. The angular distribution of this IAS, excited by the simple τ operator of the Fermi transition, also showed the $\Delta L = 0$ character as we see in Fig. 2. It is expected that the Fermi strength is concentrated in the transition to this IAS. Therefore, it is very probable that other states populated in $\Delta L = 0$ transitions are GT states [4].

TABLE II. States observed in the ^{42}Ca(^{3}He,t)^{42}Sc reaction between $E_x = 4.5$ and 8.5 MeV. The E_x values obtained for close multiplet states can have larger uncertainties than the values mentioned in the text. Less accurate E_x values are indicated by parentheses. Less accurate $\Delta L = 0$ assignments are indicated by parentheses. Observed counts of states in the angle range $\Theta = 0^\circ$–0.5° are shown as "Counts (0°)." The B(GT) values are given for the states populated in $\Delta L = 0$ transitions.

(^{3}He,t)			
E_x (MeV)	ΔL	Counts (0°)	B(GT)
(4.590)		364(46)	
(4.619)		560(52)	
4.821		435(33)	
4.873		3680(86)	
4.928	0	2117(67)	0.020(1)
5.094		532(35)	
5.143	0	2269(66)	0.021(1)
(5.686)	(0)	483(51)	0.005(1)
(5.716)	0	1221(63)	0.012(1)
5.803		1268(64)	
5.958		573(38)	
6.007		1804(71)	
6.078		516(40)	
6.167		1085(59)	
6.327	0	1924(70)	0.018(1)
6.364		567(57)	
6.737		1100(50)	
7.068		1241(58)	
7.129		476(62)	
7.261		876(78)	
7.295		830(57)	
7.418		2988(83)	
7.491		653(57)	
7.586		430(37)	
7.678		441(38)	
7.776		2094(68)	
7.884		543(64)	
7.923		2313(76)	
7.974		1503(62)	
8.105	(0)	458(42)	0.004(1)
8.182		835(70)	
8.251		1152(59)	
8.292		520(47)	
8.338		522(49)	
8.373		418(65)	
8.400		1239(79)	
8.492		431(57)	

C. Gamow-Teller transition strength

The idea of isospin symmetry comes from the fact that protons and neutrons behave almost identically in terms of the strong interaction that plays a major role in the formation of nuclear structure. Under the assumption of isospin symmetry, an analogous structure is expected for nuclei with the same A but having different T_z (isobars) [4,39,40]. The corresponding states in isobars are called IASs (or simply analog states), and transitions between corresponding analog states

TABLE III. States observed in the ^{42}Ca(^{3}He,t)^{42}Sc reaction between $E_x = 8.5$ and 11 MeV. For details, see the caption to Table II.

(^{3}He,t)			
E_x (MeV)	ΔL	Counts (0°)	B(GT)
(8.540)		749(216)	
8.664[a]		571(66)	
8.732	(0)	754(47)	0.007(1)
8.810		1492(60)	
8.854		1020(62)	
8.887		1710(72)	
8.929		1537(80)	
8.981	(0)	801(116)	0.008(1)
(9.068)		549(164)	
(9.088)		792(149)	
(9.113)		491(100)	
9.156		643(48)	
9.203		1291(66)	
9.236		1044(63)	
(9.280)		551(56)	
(9.312)		1106(64)	
9.406		916(67)	
9.437[b]		991(105)	
9.565		524(47)	
9.611		651(49)	
(9.793)		858(64)	
(9.826)		1124(69)	
9.874		620(75)	
9.901		888(79)	
(9.947)		953(75)	
(9.978)		1436(88)	
10.011	0	3137(156)	0.032(2)
(10.118)		1241(155)	
(10.142)		2324(184)	
(10.165)		1726(195)	
(10.195)		670(86)	
(10.250)	0	1651(174)	0.017(2)
(10.271)		822(171)	
10.338	0	1530(69)	0.016(1)
10.395		556(56)	
10.437	0	1956(78)	0.020(1)
10.561	(0)	604(55)	0.006(1)
10.639[c]		1163(88)	
10.695		670(59)	
10.735		466(61)	
10.809		495(70)	

[a]Identified as the ^{40}Sc, 0.772-MeV, $J^\pi = 2^-$ state.
[b]Identified as the ^{16}F, 0.424-MeV, $J^\pi = 2^-$ state.
[c]Identified as the ^{40}Sc, 2.745-MeV, $J^\pi = 1^+$ state.

(analogous transitions) have corresponding strengths. Under the assumption of isospin symmetry in the $A = 42$ isobars, which is schematically shown in Fig. 3, the corresponding $T_z = \pm 1 \rightarrow 0$ GT transitions (mirror GT transitions) observed in the ^{42}Ca(^{3}He,t)^{42}Sc reaction and the ^{42}Ti $\rightarrow$ ^{42}Sc β^+ decay are analogous and have the same B(GT) values.

Counts of individual states in the $\Theta \leqslant 0.5°$ angle cut obtained in the peak-decomposition analysis are shown as

TABLE IV. States observed in the ^{42}Ca(^{3}He,t)^{42}Sc reaction between $E_x = 11$ and 13 MeV. Only well-observed states are listed. In this region, a complete separation of states was difficult and some states have larger widths. Therefore, the determination of the peak position was less accurate and the E_x values can have an uncertainty larger than the 10 keV mentioned in the text. Observed counts of states in the angle range $\Theta = 0°$–$0.5°$ are shown as "Counts (0°)." The B(GT) values are given for the states possibly populated in $\Delta L = 0$ transitions.

(^{3}He,t)			
E_x (MeV)	ΔL	Counts (0°)	B(GT)
10.95[a]		3101(168)	
11.07		1273(89)	
11.18		623(59)	
11.22		745(745)	
11.26		852(59)	
11.40		1566(76)	
11.62		617(96)	
11.81		614(207)	
11.83	(0)	964(232)	0.010(2)
12.00	(0)	963(77)	0.010(1)
12.25[b]		650(58)	
12.42		631(82)	
12.70		640(195)	

[a]Identified as the ^{12}N, $J^\pi = 1^+$ g.s.
[b]Identified as the ^{40}Sc, $J^\pi = 0^+$, 4.368-MeV state.

"Counts (0°)" in Tables I–IV. The reduced GT transition strength B(GT) can be derived for each GT state using the "Counts (0°)" and the close proportionality given by Eq. (2). To use this relationship, we need a standard B(GT) value. For this purpose, we assume isospin symmetry in the $A = 42$ isobars. We first derive the B(GT) value for the transition from the $J^\pi = 0^+$, g.s. of ^{42}Ti to the 1^+, 0.661-MeV state in ^{42}Sc

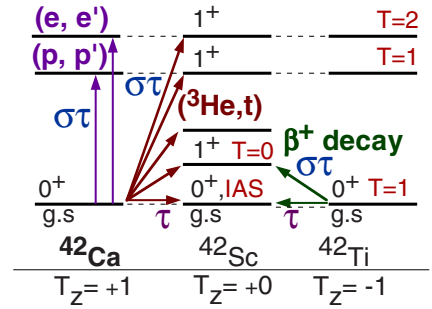

FIG. 3. (Color online) Schematic view of the analog states (connected by dashed lines) and analogous transitions in the mass $A = 42$, $T_z = +1$, 0, and -1 isobaric system. The Coulomb displacement energies are removed so that the isospin symmetry becomes clear. In this scheme, the inclined arrows show the $0^+ \rightarrow 1^+$ GT transitions caused by the $\sigma\tau$-type operator from the g.s.s of mirror nuclei ^{42}Ca and ^{42}Ti. However, the analogous $0^+ \rightarrow 0^+$ Fermi transitions to the IAS caused by the τ-type operator are shown by the horizontal arrows. The vertical arrows show the $0^+ \rightarrow 1^+$ transitions caused by inelastic-type reactions such as (p,p') or (e,e') on ^{42}Ca.

TABLE V. The properties of the transition from the g.s. of ^{42}Ti to the 0.611-MeV state in ^{42}Sc studied in the ^{42}Ti $\rightarrow$ ^{42}Sc β^+ decay. The total half-life $T_{1/2}$, branching ratio BR, and decay Q value (Q_{EC} value) used for the calculation of B(GT) values are listed.

	$T_{1/2}$ (ms)	BR (%)	Q_{EC} (keV)	B(GT)
Kurtukian[a]	208.14(45)	51.1(11)	7016.83(25)	2.157(50)
Molina[b]	211.7(19)	55.9(36)	7016.48(22)	2.313(148)

[a]From Ref. [41].
[b]From Ref. [19].

using the ^{42}Ti β-decay data. Then this B(GT) value is used to derive the unit GT cross section in Eq. (2).

Recently, two sets of accurate ^{42}Ti β-decay data became available [19,41] at the fragment separator and trap facilities. Using the β-decay half-life $T_{1/2}$, branching ratio BR, and decay Q value (Q_{EC} value) listed in Table V, the B(GT) value for the transition from the g.s. to the 0.611-MeV state was calculated for each set of ^{42}Ti β-decay data using the relationship

$$B(\mathrm{GT}) = K/(\lambda^2 f t), \tag{3}$$

where $K = 6143.6(17)$ [42], $\lambda = g_A/g_V = -1.270(3)$ [43], f is the phase-space factor calculated using the decay Q value, and t is the partial half-life determined by the values $T_{1/2}$ and BR. Taking the average of the two B(GT) values, we get $B(\mathrm{GT}) = 2.173(47)$. As mentioned, this B(GT) value is used as a standard to derive the unit GT cross section in Eq. (2) assuming the mirror symmetry in the $A = 42$ isobar system.

This assumption can bring some systematic uncertainties to the (^{3}He,t) B(GT) values, although this is probably the best we can do. Note that both the Coulomb force and charge-dependent nuclear forces can cause asymmetry in the strengths of mirror GT transitions. There is a discussion on the asymmetry of allowed GT β-decay rates in light p- and sd-shell mirror nuclei [44]. However, a quantitative estimation or an experimental study of the asymmetry for pf-shell nuclei is not available. As an extreme example, a large asymmetry for the $T_z = \pm 2 \rightarrow \pm 1$ mirror GT transitions in $A = 40$ isobars is discussed in Ref. [45].

The B(GT) values of other GT states can be calculated using the close proportionality given in Eq. (2). To evaluate the E_x dependence of $F(q,\omega)$, a DWBA calculation was performed for the ^{42}Ca(^{3}He,t)^{42}Sc reaction using the computer code DW81 [46] following the procedure discussed in Refs. [47–49]. The optical potential parameters were taken from Ref. [50]. We considered two possible transitions, $\nu f_{7/2} \rightarrow \pi f_{7/2}$ and $\nu f_{7/2} \rightarrow \pi f_{5/2}$. The calculations show that $F(q,\omega)$ decreases gradually with excitation energy. The amount of decrease was about 4%, 9%, and 16% at $E_x = 4$, 8, and 12 MeV, respectively. For both transitions, the amount of decrease was similar.

The uncertainty of a B(GT) value includes the uncertainty of the standard B(GT) value and that of the experimental count for each state in the $\Theta \leqslant 0.5^\circ$ cut [see the column "Counts (0°)" of Tables I–IV]. The uncertainty of the value "Counts (0°)" includes the statistical uncertainty and the uncertainties in the peak-decomposition analysis, but not the uncertainties associated with the subtraction of the continuum caused by the QFS process. Owing to this process, the continuous counts gradually increase above $E_x \approx 5.5$ MeV [see Fig. 1(b)]. As we see from the enlarged 0°, (^{3}He,t) spectrum of the $E_x \geqslant 6.5$-MeV region shown in Fig. 5(a) (see Sec. IV), the peak-to-continuum ratio becomes smaller as E_x increases. Therefore, we expect an additional ≈10%–15% uncertainty of B(GT) values for the states in the 8–9-MeV region, ≈15%–20% uncertainty in the 9–11-MeV region, and ≈25% uncertainty in the region above 11 MeV.

Possible effects of the tensor-isospin ($T\tau$) interaction, which can contribute in the excitation of $J^\pi = 1^+$ states with the $\sigma\tau$ interaction, can add additional systematic uncertainty in the derived B(GT) values using Eq. (2). Because the contributions from these two interactions are coherent, there is no way to extract only the $\sigma\tau$ part of the contribution experimentally. In addition, the amount of $T\tau$ contribution is dependent on the configurations of individual states. The $T\tau$ term of the nuclear interaction has the minimum strength at $q = 0$ (i.e., $\Theta \approx 0^\circ$), while the $\sigma\tau$ term has the maximum strength [51]. Therefore, the tensor contribution is usually small in the excitations of stronger 1^+ states in the 0° measurement. However, it can be relatively large for weaker states [18]. Recently, the B(GT) values of analogous $T_z = \pm 1 \rightarrow 0$ GT transitions obtained from (^{3}He,t) reactions and β decays, respectively, were compared up to the excitation energies of ≈4.5 MeV for $A = 46$, 50, and 54 isobars [19]. Note that the β decay is not contaminated by the $T\tau$ interaction. It was found that the B(GT) values of individual pairs can have differences of a few to 10%, but the cumulative GT strengths were rather similar. A theoretical estimation of the $T\tau$ contribution is given in Ref. [16].

D. Excitations from contaminant isotopes

As mentioned, the main contaminant isotope in the target was ^{40}Ca (5.1%). To identify the ^{40}Sc states in the ^{42}Sc spectrum, we recorded the 0°, (^{3}He,t) spectrum from an enriched ^{40}Ca target under the same experimental conditions as for the ^{42}Ca target. As a result, excitations of the $J^\pi = 2^-$, 0.772-MeV state, 1^+, 2.754-MeV state, and 0^+, 4.368-MeV state in ^{40}Sc [52] were identified [see Fig. 5(a) in Sec. IV]. Owing to the large difference in the reaction Q values, these states are observed at $E_x \approx 8.66$, 10.64, and 12.25 MeV, respectively, in the ^{42}Sc spectrum (see Tables III and IV). The $J^\pi = 2^-$, 0.44-MeV state in ^{16}F and the $J^\pi = 1^+$, g.s. in ^{12}N from ^{16}O and ^{12}C contaminants, respectively, were also identified in the similar energy region.

The other contaminant isotopes were ^{44}Ca (0.87%) and ^{43}Ca (0.33%). Because the IASs from these Ca isotopes have almost the same reaction Q values, the contributions of Fermi excitations from the ^{44}Ca and ^{43}Ca g.s.s to the IASs in ^{44}Sc and ^{43}Sc, respectively, are also included in the observed IAS peak. These contributions were calculated assuming that the total B(F) strength of $N - Z$ is carried by the IAS peak. Then they were subtracted (≈2.7%) from the observed peak count of the 0^+, g.s. (IAS). It is also expected that the strength of the GT excitation from the odd-mass isotope ^{43}Ca mixes with the Fermi strength incoherently. Although this contribution is expected to be small considering the small isotopic ratio of 0.33% for ^{43}Ca, we could not estimate it properly. We

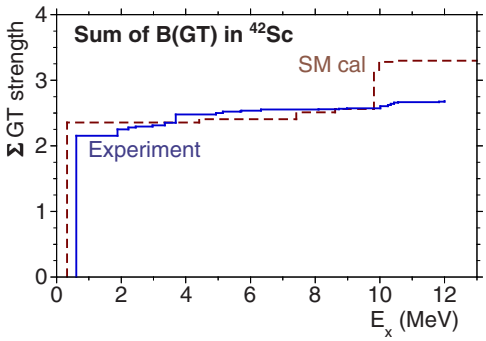

FIG. 4. (Color online) A comparison of the cumulative sums (CSs) of B(GT) strengths from the experimental ^{42}Ca(^{3}He,t)^{42}Sc measurement and the SM calculation using the effective interaction GXPF1J. A quenching factor of $(0.74)^2$ is included in the SM calculation.

also found that 2.223-, 3.224-, and 3.393-MeV peaks are contaminated by the ^{44}Sc GT excitations by comparing the present ^{42}Sc spectrum with that of the ^{44}Ca(^{3}He,t)^{44}Sc reaction given in Ref. [32]. Their contributions were subtracted referring to the ^{44}Sc spectrum.

IV. DISCUSSION

A. Gamow-Teller strength distribution

The experimental B(GT) distribution in ^{42}Sc studied up to 12 MeV is shown in Fig. 4 in the form of a cumulative sum (CS). A total B(GT) value of 2.7(4) has been obtained, where most of the strength (≈80%) is concentrated in the lowest 0.611-MeV GT state. The B(GT) distribution from a SM calculation is also shown in Fig. 4. The calculation was performed using the GXPF1J interaction [53,54]. The model space was restricted to the pf shell and an inert ^{40}Ca core was assumed. The B(GT) values shown include the quenching factor of $(0.74)^2$ inherent in the SM calculations for pf-shell nuclei [54].

The SM calculation reproduces the concentration of the B(GT) strength to the lowest GT state and the overall B(GT) distribution, but not the fragmented strengths between 2 and 6 MeV. It is suggested that the fragmentation in this region is caused by the mixing with the sd-shell configurations resulting from g.s. correlations (see also the discussions in Refs. [22,32]). Note that this effect is not included in our SM calculation, because we assume an inert ^{40}Ca core. In addition, in the SM calculation, we see a sudden increase of the CS strength owing to the $T = 1$ state predicted at $E_x = 9.82$ MeV with a relatively large B(GT) value of 0.6 (see Fig. 4). This is the lowest $T = T_0 = 1$ GT state, where T_0 is the T value of the g.s. of the initial nucleus, and all lower E_x states have $T = 0$. A $T = 1$ GT state with B(GT) = 0.44 is also predicted at 9.1 MeV in a SM calculation using the KB3G interaction [55]. In the experiment, however, we only observed several weakly excited states with B(GT) values of 0.01–0.03 in the 10.0–10.6-MeV region, although some of the weakly excited states may not have been detected in the experiment.

The Ikeda sum rule for GT strengths in nuclei is expressed by $\Sigma B(\mathrm{GT}_-) - \Sigma B(\mathrm{GT}_+) = 3(N - Z)$, where $\Sigma B(\mathrm{GT}_-)$ and $\Sigma B(\mathrm{GT}_+)$ are sums of GT$_-$ and GT$_+$ transition strengths measured by (p,n)- and (n,p)-type reactions, respectively [2,56]. The quenching of the GT strength compared to the Ikeda sum rule has been a matter of considerable discussion and interest in nuclear physics [2,57].

Because the neutron excess in the target nucleus ^{42}Ca is 2, the value of $3 \times (N - Z)$ is 6. The total sum of the B(GT) strengths experimentally observed in the transitions to discrete states up to 12 MeV is 2.7(4), that is 45% of 6. Owing to the nature of LS shell closure at $Z = 20$, it is expected that the strength $\Sigma B(\mathrm{GT}_+)$ in the (n,p) direction, i.e., the $T = T_0 + 1 = 2$ strength, is zero (or very small) owing to the Pauli exclusion principle. Assuming isospin symmetry, the $T = 2$ strength in the (p,n) direction is also almost zero. Therefore, our result suggests that the total sum of the B(GT) strength located in fragmented discrete states in the E_x region up to 12 MeV is less than half of the sum-rule-limit value. A small summed GT strength of ≈40% compared to the Ikeda sum rule is also reported in the ^{44}Ca(^{3}He,t)^{44}Sc measurement analyzed up to $E_x \approx 14$ MeV [32]. Similarly, in a recent analysis of the ^{48}Ca(p,n)^{48}Sc measurement performed up to a higher E_x of ≈30 MeV, a relatively small total GT strength of ≈65% of the sum-rule-limit value was suggested even if the $\Delta L = 0$ strength in the continuum caused by the QFS is included [58]. It seems that the "quenching" of the GT strength is still an abiding issue to be studied and discussed.

B. Isospin T of states populated in Gamow-Teller transitions

We identified GT states excited with B(GT) values of 0.01–0.03 in the $E_x = 10$–12-MeV region. Here we deduce the isospin value T of these GT states by examining the existence of corresponding states, i.e., analog spin-$M1$ states, in the ^{42}Ca(p,p') spectrum measured at 0° and $E_p = 200$ MeV [59]. For this purpose, first the properties and isospin structure of spin-$M1$ and GT excitations are briefly summarized. For the details, see Refs. [4,32,60].

In (p,p') reactions at intermediate energies, spin-$M1$ states excited by $M1_\sigma$ transitions caused either by the σ operator or the $\sigma\tau$ operator become prominent at 0° [2,51]. If the $M1_\sigma$ transitions start from the 0^+ g.s. of even-even nuclei with the isospin value $T = T_0 \geqslant 1$, they are mainly caused by the $\sigma\tau$ operator [2,4,51] and have the IV nature. Then, similar to Eqs. (1) and (2), we can expect a close proportionality between the 0° cross section of a spin-$M1$ state and the reduced $M1_\sigma$ transition strength $B(M1_\sigma)$,

$$\sigma^{M1\sigma}(q,\omega) \simeq K(\omega) N_{\sigma\tau} |J_{\sigma\tau}(q)|^2 B(M1_\sigma) \quad (4)$$

$$= \hat{\sigma}^{M1\sigma} F(q,\omega) B(M1_\sigma), \quad (5)$$

where $\hat{\sigma}^{M1\sigma}$ is the unit cross section for the $M1_\sigma$ transition. Owing to the close proportionality in both (^{3}He,t) and (p,p') reactions, it is expected that the analog GT and spin-$M1$ states are excited with corresponding strengths.

In (p,p') measurements, it is reported that the $J^\pi = 1^+$ spin-$M1$ states in the even-even pf-shell nuclei are observed in the $E_x = 7$–14-MeV region [61–63]. Furthermore, by comparing the (p,p') and (^{3}He,t) spectra measured at 0°,

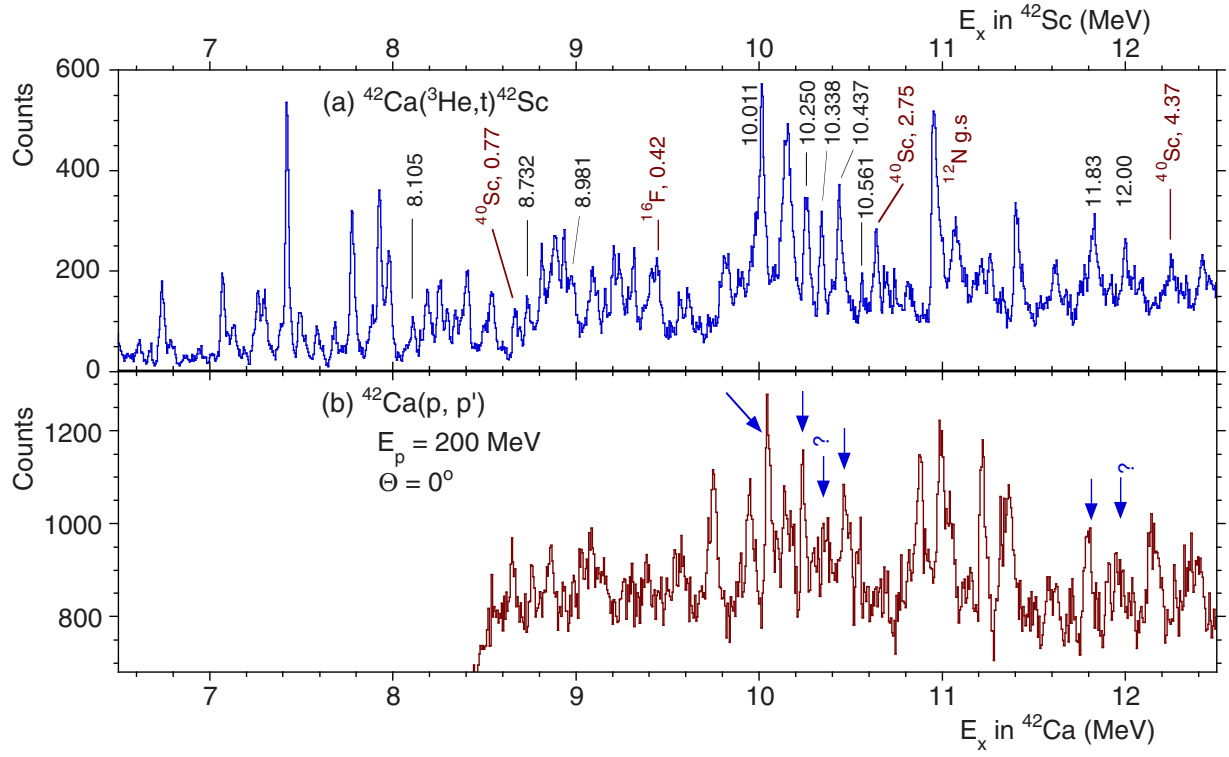

FIG. 5. (Color online) (a) The ^{42}Ca(^{3}He,t) spectrum of the $E_x = 6.5$–12.5-MeV region for events with scattering angles $\Theta \leqslant 0.5^\circ$. The counts of the continuum caused by the quasifree scattering (QFS) increase, in particular, in the $E_x = 8$–11-MeV region. States with or probably with $\Delta L = 0$ are indicated by their excitation energies. States originated from ^{40}Ca, ^{16}O, and ^{12}C contaminants in the ^{42}Ca target are also indicated. (b) The IUCF ^{42}Ca(p,p') spectrum measured at $E_p = 200$ MeV [59]. The measurements were carried out at very forward angles including 0° using the K600 spectrometer in transmission mode [64]. The $E_x > 8.5$-MeV region in ^{42}Ca was studied. The peaks corresponding to the $\Delta L = 0$ states in the (^{3}He,t) spectrum are shown by arrows. The vertical scales are adjusted so that the 10.011-MeV state in the (^{3}He,t) spectrum and the corresponding state in the (p,p') spectrum have nearly the same heights. Note that the ordinate of the ^{42}Ca(p,p') spectrum begins with a finite count to illustrate the structured part clearly.

corresponding states, i.e., isospin analog states, populated in $M1_\sigma$ and GT transitions starting from $T_z = +1$ pf-shell nuclei ^{58}Ni and ^{54}Fe have been studied in detail for the ^{58}Ni and ^{58}Cu pair and the ^{54}Fe and ^{54}Co pair, respectively [20,21]. As a result, it was found that the GT states with $T = T_0 = 1$ are located mainly in the $E_x = 8.5$–11.5-MeV region in the final $T_z = 0$ nuclei ^{58}Cu and ^{54}Co, while the $T = T_0 + 1 = 2$ states lie in the higher 10–13-MeV region. It should be noted that higher T states are expected at higher energies owing to the symmetry energy [40,60].

The spin-$M1$ states observed in the ^{42}Ca(p,p') reaction can have isospin values of either $T = T_0 = 1$ or $T = T_0 + 1 = 2$. As shown schematically in Fig. 3, these $T = 1$ and 2 spin-$M1$ states in ^{42}Ca are analogous to the $T = 1$ and 2 GT states in ^{42}Sc, respectively, under the assumption of isospin symmetry. Therefore, for the identification of analogous structures and the analog states in ^{42}Sc and ^{42}Ca, it is best to compare the spectra from the ^{42}Ca(^{3}He,t)^{42}Sc and ^{42}Ca(p,p') reactions at 0°, where GT states and spin-$M1$ states, respectively, are prominent owing to their $\Delta L = 0$ character.

The detail of the $E_x = 6.5$–12.5-MeV region of the 0°, ^{42}Ca(^{3}He,t)^{42}Sc spectrum is shown in Fig. 5(a), where the states populated (and probably populated) in $\Delta L = 0$ transitions are labeled by their E_x values. They are the candidates for the GT states of interest.

In Ref. [59], a ^{42}Ca(p,p') spectrum taken at very forward angles including 0° is presented. The experiment was carried out at Indiana University Cyclotron facility (IUCF), Indiana, using the K600 magnetic spectrometer and a 200-MeV proton beam. A self-supporting ^{42}Ca target with an enrichment of 93.71% and an areal density of 3.5(5) mg/cm^2 was placed in the scattering chamber of the spectrometer. The transmission mode of the K600 spectrometer, where the incoming proton beam directly passes through the spectrometer, was used in the measurement [64]. As a result, the region above the threshold energy of 8.5 MeV in ^{42}Ca could be studied as shown in Fig. 5(b).

The E_x scale of the ^{42}Ca(p,p') spectrum was determined referring to the E_x values of known spin-$M1$ states observed in the ^{28}Si(p,p') spectrum taken under the same conditions and shown in Ref. [59]. The E_x scale can have a systematic uncertainty of ≈30–50 keV. The analog state of the g.s. of ^{42}Ca (IAS) is the g.s. in ^{42}Sc. Therefore, the same energy scale is used in Figs. 5(a) and 5(b).

It is known that in (p,p') reactions at intermediate incident energies and 0°, not only the spin-$M1$ states, but also the Coulomb excited $E1$ states, i.e., the $J^\pi = 1^-$ states excited by $E1$ transitions, can be rather prominent [5]. Therefore, a high selectivity for the spin-$M1$ states is not always guaranteed. However, at least for the four clear $\Delta L = 0$ states identified

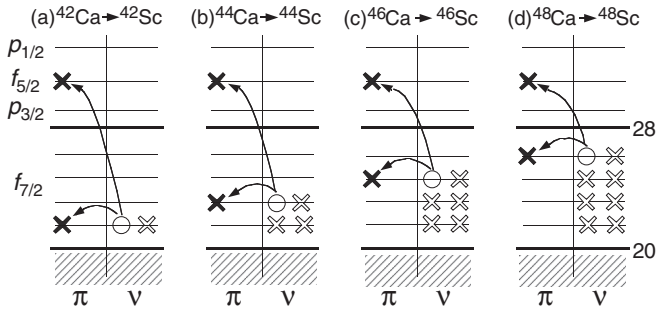

FIG. 6. The SM configurations before and after the β^--type GT transitions in $A = 42$–48 Ca isotopes. Positions occupied by neutrons (ν) are shown by open crosses. Positions that are newly occupied by protons and unoccupied by neutrons after making GT transitions (shown by the arrows) are indicated by solid crosses and open circles, respectively. The shell closures at $Z = N = 20$ and 28 are indicated by thick solid lines.

by their excitation energies in the 10.0–10.5-MeV region of the (^{3}He ,t) spectrum, corresponding sharp peaks are found in the (p,p') spectrum [peaks shown by arrows in Fig. 5(b)], although all of these states are weakly excited. Because the ratios of the strengths of corresponding peaks are more or less the same, we suggest that they are the candidates for analog states with an identical T value of either $T = 1$ or $T = 2$.

As discussed, from a simple SM picture of ^{42}Ca with the $Z = 20$ proton LS-closed shell [see Fig. 6(a)], GT transitions to the $T = 2$ states in the $T_z = +2$ ^{42}K nucleus are not allowed. Therefore, the analog $T = 2$ GT states in ^{42}Sc are also not excited in the (p,n)-type reactions. In addition, $T = 2$ states are situated higher in energy than the $T = 1$ states. We also note that for a $T_0 = 1$ target nucleus such as ^{42}Ca the excitation of $T = 2$ GT states is suppressed by a factor of 3 in the (^{3}He ,t) reaction compared to the corresponding spin-$M1$ states observed in the (p,p') reaction owing to the different Clebsch-Gordan coefficients [4]. Taking these considerations into account, we suggest that these four $\Delta L = 0$ states in the 10.0–10.5-MeV region have $T = T_0 = 1$. As discussed in Sec. IV A, the results of the SM calculation are also in favor of the $T = 1$ assignments.

We give a tentative $\Delta L = 0$ assignment to the wider states at 11.83 and 12.00 MeV. It appears that there are corresponding states in the (p,p') spectrum. Thus, they are also the candidates for the $T = 1$ states. However, further discussions on these states situated in the region of high level-density is difficult, because it is hard to judge whether they really have widths or they are multiple states.

As we see in Table III, all of the candidates for the $T = 1$ GT states are weakly excited. We can partly attribute the weak strengths to the shell structure of the final nucleus ^{42}Sc having "π particle-ν particle (πp-νp)" nature. Taking the antisymmetrization principle for a particle-particle (p-p) configuration into account, we notice that the ($\pi f_{7/2}$, $\nu f_{7/2}$), p-p configuration cannot form the $T = 1$, $J = 1$ coupling. Only the ($\pi f_{5/2}$, $\nu f_{7/2}$), p-p configuration can contribute to the excitation of the $T = 1$ states. However, the observed total strength of the $T = 1$ GT excitation is much weaker than is expected in the $\nu f_{7/2} \rightarrow \pi f_{5/2}$ transition. In addition, the GT strength in the 10–12-MeV region is much weaker than that observed in the same region in the $A = 54$ [20] or $A = 58$ [21] systems, where GTR structures were observed. The weak strength cannot be fully understood on the discussion assuming the simple shell structure mentioned above. For further understanding, it was found that the effect of an attractive residual isoscalar (IS) interaction that is active among πp-νp configurations should be taken into account [7]. This subject is discussed in the following section (Sec. IV C).

A state excited in an $M1$ transition with a strength of $B(M1) = 0.59(5)\mu_N^2$ is reported at 11.235 MeV in an electron inelastic scattering experiment on a ^{42}Ca target [65]. This $B(M1)$ value corresponds to the excitation with a $B(\mathrm{GT}) \approx 0.19$ [4] in the ^{42}Ca(^{3}He ,t)^{42}Sc reaction if we assume that the 11.235-MeV state has $T = T_0 = 1$ and that the state is mainly excited by the $\sigma\tau$ term of the electromagnetic $M1$ operator. As we see from Table IV, and also from Fig. 5, no corresponding state with this large $B(\mathrm{GT})$ is observed either in the present (^{3}He ,t) reaction or in the (p,p') measurement. Note that the electromagnetic $M1$ operator has the orbital term in addition to the spin term [4]. Whether the contribution of the orbital term can explain this strong $M1$ excitation or not is an interesting question.

C. Excitation of a "low-energy super-Gamow-Teller state"

1. Formation of low-energy collective Gamow-Teller state

A simple SM picture of ^{42}Ca is that two valence neutrons are in the $f_{7/2}$ shell on top of the core of ^{40}Ca. Therefore, GT excitations caused by the $\nu f_{7/2} \rightarrow \pi f_{7/2}$ and $\nu f_{7/2} \rightarrow \pi f_{5/2}$ transitions, respectively, are expected in the low-energy region and in the region about 5–6 MeV higher, corresponding to the energy difference of the $j_<, \pi f_{5/2}$ shell and the $j_>, \pi f_{7/2}$ shell. However, as is clear in Fig. 4, the low-lying 0.611-MeV GT state collects the main part (≈80%) of the GT strength in the region up to 12 MeV, where the analysis was performed. In addition, in the $E_x = 5$–6-MeV region, no prominent strength corresponding to the $\nu f_{7/2} \rightarrow \pi f_{5/2}$ transition was found. As mentioned, the ^{42}Ca(^{3}He ,t)^{42}Sc spectrum at 0° was continuous and flat above 12 MeV up to 25 MeV, suggesting that the strength caused by the QFS is dominant.

As discussed, bumplike GTRs with $E_x = 9$–16 MeV and a few-MeV width have been systematically observed in nuclei with mass A larger than ≈50 in the studies of (p,n) reactions [10,11]. Note that GTRs were always observed at excitation energies higher than the energy difference of the $j_<$ and $j_>$ shells. In addition, they found that the GTRs carried the main part (≈50%–60%) of the total GT sum-rule strength and the strength in the low-energy region was always smaller.

In larger A stable target nuclei that were studied in these (p,n) reactions, the neutron number N is always greater than the proton number Z. Owing to the neutron excess, the main configurations of the GTRs are always of "π particle-ν hole (πp-νh)" nature. It is well established that the effective residual interactions among the particle-hole (p-h) configurations have an IV and repulsive nature in IV excitations such as GT or IV dipole excitations. The residual interactions make the

TABLE VI. Results of the pf-shell SM calculation using the GXPF1J interaction. The matrix elements M(GT) of GT transitions exciting individual $J^\pi = 1^+$ GT states in ^{42}Sc from the g.s. of ^{42}Ca are shown for each configuration. The results are shown for all excited GT states predicted in the region up to 9.82 MeV. The notation $f7 \rightarrow f7$, for example, stands for the transition with the $\nu f_{7/2} \rightarrow \pi f_{7/2}$ type and $p3 \rightarrow p3$ the $\nu p_{3/2} \rightarrow \pi p_{3/2}$. The summed value of the matrix elements is denoted by ΣM(GT) and its squared value is the B(GT), where the B(GT) values do not include the quenching factor of the SM calculation.

States in ^{42}Sc		Configurations						Transition strengths	
E_x (MeV)	T	$f7 \rightarrow f7$	$f7 \rightarrow f5$	$f5 \rightarrow f7$	$p3 \rightarrow p3$	$p3 \rightarrow p1$	$p1 \rightarrow p3$	ΣM(GT)	B(GT)
0.33	0	1.383	0.548	0.063	0.031	0.024	0.016	2.07	4.28
4.41	0	0.719	−0.742	−0.085	−0.079	−0.073	−0.048	−0.31	0.09
7.41	0	0.193	−0.788	−0.090	0.142	0.060	0.040	−0.44	0.19
8.62	0	−0.151	0.385	0.044	0.109	−0.071	−0.047	0.30	0.09
9.82	1	0.0	1.196	−0.137	0.0	−0.053	0.035	1.04	1.08

contributions of the transition matrix elements associated with the formation of these p-h configurations in phase. As a result, the IV giant resonances (GRs) have a collective nature. In addition, owing to the repulsive nature of the active residual interactions, IV GRs, including GTRs, are pushed up in their excitation energies relative to the unperturbed p-h energies [5].

However, we notice that the GT states in ^{42}Sc have a "πp-νp" nature consisting of $(\pi f_{7/2}, \nu f_{7/2})$ and $(\pi f_{5/2}, \nu f_{7/2})$ configurations [see Fig. 6(a)]. Naturally, they are formed by the CE-type $\nu f_{7/2} \rightarrow \pi f_{7/2}$ and $\nu f_{7/2} \rightarrow \pi f_{5/2}$ transitions starting from the naive image of ^{42}Ca with two $f_{7/2}$ neutrons on top of the $N = Z = 20$, LS-closed ^{40}Ca core. (In reality, this image is too simple; see Sec. IV C 2 and Table VI.) As discussed in Ref. [7], the contributions of the matrix elements that form these πp-νp configurations become in phase owing to the attractive IS-type residual interaction and thus a collective GT state appears at a low E_x of 0.611 MeV.

Pairing correlations between nucleons play an essential role in the formation of nuclear structure [6]. The studies have been mainly directed to the IV spin-singlet ($T = 1$, $S = 0$) channel, and it is known that the $J^\pi = 0^+$ nature of the g.s. of even-even nuclei is explained by the attraction between identical nucleons.

Interest is also directed to the IS spin-triplet ($T = 0$, $S = 1$) channel. It is discussed that the attraction between neutrons and protons is even stronger in the IS spin-triplet channel, which gives rise to a bound $J^\pi = 1^+$ g.s. in deuteron. It is also discussed that the contribution of the IS spin-triplet interaction can be observed clearly in nuclei with $N \approx Z$ [66,67]. Accordingly, in theoretical calculations attempts have been made to include the IS-type residual interactions for the study of ^{42}Ca $\rightarrow$ ^{42}Sc GT transitions. In a spherical quasiparticle random-phase approximation (QRPA) calculation including the IS residual interaction in addition to the IV residual interaction [8], it is suggested that not only the $(\pi f_{7/2}, \nu f_{7/2})$ and $(\pi f_{5/2}, \nu f_{7/2})$ configurations mentioned above, but also a configuration produced by the $\nu f_{5/2} \rightarrow \pi f_{7/2}$ transition makes an additional in-phase contribution, which increases the collectivity of the lowest 1^+ GT state in ^{42}Sc.

As a consequence of the strongly attractive proton-neutron (π-ν) interaction in the IS spin-triplet channel, a possible IS pairing condensate in heavy $N \simeq Z$ nuclei has been theoretically discussed [66,68–70]. It should be noted that the IS pairing condensate, if it exists, is unique to nuclei consisting of two kinds of fermions, i.e., protons and neutrons. In the $\pi\nu$ p-p random-phase approximation (ppRPA) calculation [71], it is suggested that the lowest $J^\pi = 1^+$ state in ^{42}Sc can be a precursory soft mode of the IS pairing condensation. Their calculation also showed that the lowest 1^+ state in ^{42}Sc is mainly constructed by the in-phase excitation of the πp-νp configurations involving the f-shell orbits. On top of that, they found that the collective nature is enhanced by the in-phase contribution of the $p_{3/2}$ orbits above the Fermi levels and also by the contribution of the π hole-ν hole (πh-νh) configurations of sd-shell orbits below the Fermi levels. These contributions of the $p_{3/2}$ and sd-shell orbits, however, are rather small [71].

2. *Configurations calculated in the shell model*

As shown in Fig. 4, the SM calculation in the pf-SM space using the GXPF1J interaction [53,54] reproduces the strong GT transition strength to the lowest $T = 0$, 1^+ state calculated at $E_x = 0.33$ MeV. It also reproduces the weak GT strengths to all three $T = 0$ states situated between this 0.33-MeV state and the $T = 1$ GT state at 9.82 MeV.

We examine the configurations and the values of GT matrix elements for each of these four $T = 0$ states and also for the $T = 1$ state at 9.82 MeV. They are listed in Table VI. In the lowest 1^+ state predicted at 0.33 MeV, we see that not only the matrix elements of the main configurations of $\nu f_{7/2} \rightarrow \pi f_{7/2}$ and $\nu f_{7/2} \rightarrow \pi f_{5/2}$, but also all other matrix elements are in phase, which makes the total value of the transition matrix element M(GT) large and thus the excitation of this state strong. Thus, the results of the RPA calculations mentioned above are confirmed.

Cancellation of matrix elements is seen in the excitations of three other $T = 0$, 1^+ states, and thus small ΣM(GT) values are predicted. This is in agreement with the experimental observation of weakly excited states in the $E_x = 1.8$–9-MeV region. However, the fragmentation of the GT strength, as discussed in Sec. IV A, is not so well reproduced. The fifth row shows the matrix elements for the excitation of the $T = 1$, 1^+ state predicted at 9.82 MeV. As we discussed in Sec. IV B, no contribution is expected from the $\nu f_{7/2} \rightarrow \pi f_{7/2}$ (and also $\nu p_{3/2} \rightarrow \pi p_{3/2}$) transition. The excitation is mainly attributable to the $\nu f_{7/2} \rightarrow \pi f_{5/2}$ matrix element.

3. *Low-energy super-Gamow-Teller states in nuclei*

In Ref. [7], the lowest $J^\pi = 1^+$ state at 0.611 MeV was named the "low-energy super-Gamow-Teller state (LESGT state)" owing to its character close to the "supermultiplet state" that was proposed by Wigner [72]. The supermultiplet state appears in the limit of a null LS force and the restoration of SU(4) symmetry. In this limit, we expect that (a) the GT strength is concentrated in a low-energy GT state and (b) excitation energies of both the IAS caused by the Fermi transition and the GT state are identical.

As was discussed, the essential requirements to form the LESGT states are that their main configurations have the property of πp-νp and that one of them have the "zero-energy" nature. Then, the attractive IS residual interaction can play an essential role to collect the available GT strengths into the LESGT state. We notice that these conditions are realized if initial even-even nuclei have either two neutrons or two protons on top of an LS-closed, $N = Z$ doubly magic nucleus and the GT transitions are to the odd-odd, $N = Z$ final nucleus. Because the LS-closed doubly magic nuclei are ^{4}He, ^{16}O, ^{40}Ca, and possibly ^{80}Zr, it is expected that the $J^\pi = 1^+$ LESGT states are strongly excited in the $T_z = 0$, $A = 6$, 18, 42, and 82 nuclei by the GT transitions starting from the neighboring $J^\pi = 0^+$ g.s. of $T_z = \pm 1$ isobars. In the $A = 6$ system, the initial nuclei are ^{6}He and ^{6}Be and the final nucleus is ^{6}Li; in the $A = 18$ system, the initial nuclei are ^{18}O and ^{18}Ne and the final nucleus is ^{18}F; in the $A = 42$ system, the initial nuclei are ^{42}Ca and ^{42}Ti and the final nucleus is ^{42}Sc; and in the $A = 82$ system, the initial nuclei are ^{82}Zr and ^{82}Mo and the final nucleus is ^{82}Nb.

In the $A = 6$ and 18 systems, strong GT transitions have been observed in the β-decay studies of $^6\text{He} \rightarrow {}^6\text{Li}$ and $^{18}\text{Ne} \rightarrow {}^{18}\text{F}$, respectively. They are from the $J^\pi = 0^+$ g.s. of initial nuclei to the $J^\pi = 1^+$ g.s. of final nuclei. These GT transitions have very small log ft values of 2.9059(7) [corresponding to the B(GT) value of 4.73(2)] and 3.091(4) [corresponding to the B(GT) value of 3.09(3)], respectively [73,74]. In addition, from the $^{18}\text{O}(p,n)^{18}\text{F}$ spectrum at 0° measured up to $E_x = 20$ MeV [75], we can confirm that the main part of the GT strength is concentrated in the g.s. of ^{18}F. Surely, both the $J^\pi = 1^+$ g.s. of ^{6}Li and ^{18}F are identified as LESGT states. In accordance with these findings, we expect that the g.s.-g.s. GT transitions in the reversed direction, i.e., the GT transitions starting from the LESGT states in these $T_z = 0$ nuclei to the $J^\pi = 0^+$ g.s. of the neighboring $T_z = \pm 1$ nuclei, are also strong. Strong GT transitions are actually observed in the $^6\text{Li}(p,n)^6\text{Be}$ reaction [76] and the $^{18}\text{F} \rightarrow {}^{18}\text{O}$ β decay [74].

It should be noted that "zero-energy" πp-νp configurations are realized only in CE excitations and β decays and never in inelastic excitations. We also see that the existence of IS and IV residual interactions, and thus, low- and high-energy GT vibrational states, i.e., LESGT states and the GTRs, respectively, are attributed to the two fermionic degrees of freedom of protons and neutrons, which is unique to atomic nuclei.

We notice that LESGT states have similar properties with the $T = 0$, $J^\pi = 1^+$ g.s. of deuteron. The analysis of the deuteron binding energy in terms of bare π-ν interactions suggests that the contribution of the D wave configuration and the tensor interaction is large [77]. We have seen that the low E_x and the collective feature of the LESGT state is caused by the attraction in the IS spin-triplet channel, in which the tensor interaction is expected to play a dominant role. How one can explain the properties of the LESGT state in terms of the tensor interaction, in a way similar to the deuteron binding, will be an intriguing but difficult subject. Note that the screening effects on the tensor interaction owing to the nuclear medium are not yet well understood. An attempt to include the effect of the bare tensor force into the effective $T = 0$, π-ν pairing interaction in finite mass nuclei is discussed in Refs. [78,79].

TABLE VII. The E_x values of the lowest-excited GT states [E_x GT$_1$] (in units of MeV), their B(GT) values [B(GT)$_1$], and the sum of the B(GT) values in the E_x < 4-MeV region [$\Sigma B(\text{GT})_{0-4}$] in ^{42}Sc, ^{44}Sc, and ^{48}Sc are compared. The ratio of the $\Sigma B(\text{GT})_{0-4}$ value and the sum-rule-limit value of $3(N - Z)$ are given as the "Ratio" in the last column.

Target	E_x GT$_1$	B(GT)$_1$	$\Sigma B(\text{GT})_{0-4}$	$3(N-Z)$	Ratio
^{42}Ca[a]	0.61	2.17	2.50	6	0.42
^{44}Ca[b]	0.67	0.71	1.88	12	0.16
^{48}Ca[c]	2.53	1.1	1.3	24	0.05

[a]Present study.
[b]From Ref. [32].
[c]From Ref. [80].

D. Gamow-Teller strength distributions in ^{42}Sc, ^{44}Sc, and ^{48}Sc

We discuss the mass A dependence of the strength distributions of GT transitions in $A = 42$, 44, and 48 scandium isotopes starting from the calcium isotopes with the corresponding mass. With high-resolution (^{3}He,t) measurements, GT transitions from the $T_z = +2$ nucleus ^{44}Ca to the $T_z = +1$ nucleus ^{44}Sc have been studied up to $E_x \approx 14$ MeV [32] and those from the $T_z = +4$ nucleus ^{48}Ca to the $T_z = +3$ nucleus ^{48}Sc up to ≈7 MeV [80]. In these studies, it was found that the GT strength was mainly in the E_x < 6-MeV region in ^{44}Sc, while in ^{48}Sc, the main part of the strength was in the GTR region of 6–15 MeV judging from the energy spectrum shown in Ref. [80]. As we have observed, the GT strength in ^{42}Sc is strongly concentrated in the lowest GT state. Here we can study how the strength moves to a higher E_x region as a function of neutron excess.

The E_x values of the lowest GT state in ^{42}Sc, ^{44}Sc, and ^{48}Sc, their B(GT) values, the summed values of B(GT) strengths in the low-E_x region of <4 MeV, and the ratios compared to the sum-rule B(GT) values of $3(N - Z)$ are summarized in Table VII. As we see, the excitation energies of the lowest GT states are higher in the higher A isotopes. The summed B(GT) values in the E_x < 4-MeV region decrease as a function of A and the ratios of the summed B(GT) values compared to the sum-rule B(GT) values decrease drastically.

In a simple SM picture, as we see in Fig. 6, only two kinds of transitions, i.e., $\nu f_{7/2} \rightarrow \pi f_{7/2}$ and $\nu f_{7/2} \rightarrow \pi f_{5/2}$, contribute to making GT transitions in all of these nuclei. We

notice that the $(\pi f_{7/2}, \nu f_{7/2})$ and $(\pi f_{5/2}, \nu f_{7/2})$ configurations in the final nucleus ^{42}Sc, as discussed in Sec. IV C, have p-p nature [Fig. 6(a)]. As A increases, however, both of these configurations gradually lose the p-p nature and acquire p-h nature. We see that they have pure p-h nature in ^{48}Sc [Fig. 6(d)].

From the mass dependence of the GT strength distributions in scandium isotopes, we can clearly see that the GT strengths consisting of p-p configurations, as in ^{42}Sc, are pulled down and mainly concentrate in the lowest energy GT state, i.e., the collective LESGT state. As discussed in Refs. [7,8], the LESGT state is formed by the attractive IS residual interaction that is active among p-p configurations. However, the GT strengths consisting of p-h configurations, as in ^{48}Sc, are pushed up to the energy region higher than the single-particle energies of individual configurations by the repulsive IV residual interaction and form the collective GTR [see the energy spectrum of ^{48}Ca(^{3}He,t)^{48}Sc reaction given in Ref. [80]]. As we discussed, the GTRs that have bumplike structures and carry the main part of the GT transition strength have been observed in all $N \gg Z$ nuclei in (p,n)-type CE reactions [4,5,10,11].

V. SUMMARY AND CONCLUSIONS

We carried out a ^{42}Ca(^{3}He,t)^{42}Sc measurement at the intermediate beam energy of 140 MeV/nucleon and scattering angles around 0°. The energy resolution of 29 keV ($\Delta E/E \approx 7 \times 10^{-5}$) allowed us to resolve many discrete states up to 12 MeV. The g.s. in ^{42}Sc is the IAS of the $J^\pi = 0^+$ g.s. of ^{42}Ca. Both this IAS and the $J^\pi = 1^+$ GT state at 0.611 MeV were prominent, but other states were weakly excited. The 0.611-MeV GT state showed a forward-peaked angular distribution typical of the $\Delta L = 0$ transition. As a result of the angular distribution analysis for other weakly excited states, it was found that about 20 states show similar angular distributions and we identify them as having a $\Delta L = 0$ nature. Assuming that all of these $\Delta L = 0$ states, except the IAS, are GT states, the reduced GT transition strengths B(GT) were derived using the proportionality between the GT cross section at 0° and the B(GT) value. The B(GT) values obtained in the ^{42}Ti β decay were used as the normalization standard assuming symmetry for the $T_z = \pm 1 \rightarrow 0$ GT transitions.

We can deduce isospin values of excited GT states in ^{42}Sc by comparing the (^{3}He,t) and (p,p') spectra on the target nucleus ^{42}Ca. Starting from the $T = T_0 = 1$, g.s. of the $T_z = +1$ nucleus ^{42}Ca, the (^{3}He,t) reaction can populate GT states with $T = 0, 1$, and 2 in ^{42}Sc. However, the ^{42}Ca(p,p') inelastic scattering can excite spin-$M1$ states with $T = 1$ and 2 in ^{42}Ca. Under the assumption that isospin is a good quantum number, these spin-$M1$ states are the analog states of the $T = 1$ and 2 GT states, respectively. By comparing the 0° spectra from these reactions, several pairs of corresponding states were identified in the 10–12-MeV region. Taking the energy systematics of the $T = 1$ and 2 GT states in final $T_z = 0$ nuclei and also the LS-closed nature of the $Z = 20$ proton shell in ^{42}Ca into account, we assigned $T = 1$ for these several pairs of weakly excited states.

About 80% of the observed GT transition strength was concentrated in the excitation of the lowest 0.611-MeV GT state. We call this state the LESGT state. The SM calculation using the GXPF1J interaction showed that several f- and p-shell configurations make an in-phase contribution in the excitation of this state. A spherical QRPA calculation showed that this state has a collective nature and the collectivity originates in the IS-type attractive interaction that is active among the p-p type configurations of the f- and higher p-shell orbits [mainly $(\pi f_{7/2}, \nu f_{7/2})$ and $(\pi f_{5/2}, \nu f_{7/2})$ configurations]. In addition, a ppRPA calculation suggested that the πh-νh configurations of the lower sd-shell orbits are also involved in the formation of the LESGT state in ^{42}Sc. As a result, it was suggested that the lowest $J^\pi = 1^+$ state in ^{42}Sc can be a precursory soft mode of the $T = 0$ pairing condensation.

The mass dependence of the GT strength distributions in scandium isotopes was examined. In a simple SM picture, it is estimated that GT states in ^{42}Sc have p-p configurations, while those in ^{48}Sc have p-h configurations. We can clearly see that the GT strength in ^{42}Sc is concentrated in the lowest energy state, i.e., the collective LESGT state. However, the GT strength in ^{48}Sc is pushed up to the energy region higher than the single-particle energies of individual configurations and forms the collective GTR. This provides a clear evidence that the attractive interaction is active in πp-νp configurations and the repulsive interaction in πp-νh configurations.

Since the finding of the IV giant dipole resonance (IV GDR) in the 1960s (see, e.g., Ref. [81]) and also of the IV $M1$ excitations in the 1980s using inelastic-type reactions, it has been known that the p-h configurations of protons and neutrons excited by IV-type inelastic scattering reactions are the stage for the repulsive IV interaction to be active. In addition, the systematic finding of GTRs in heavier $N > Z$ nuclei in (p,n)-type CE reactions supports this idea. On the contrary, we now see that the πp-νp configurations on the LS-closed magic nuclei that are realized in CE excitations and β decays starting form the nuclei with two identical nucleons on top of the LS-closed magic nuclei are the ideal stage for the attractive IS spin-triplet pairing interaction to be active; if one such configuration has the "zero-energy" nature, a low-energy collective state, the LESGT state, is formed by the attractive nature of the IS interaction.

Note that a "zero-energy" πp-νp configuration, i.e., $(\pi f_{7/2}, \nu f_{7/2})$ configuration in the ^{42}Ca $\rightarrow$ ^{42}Sc transition, is realized only in CE excitations and β decays and never in inelastic-type excitations. We also note that the existence of IS and IV residual interactions, and thus, the existence of the low-energy and high-energy collective states, i.e., the LESGT state and the GTR, are attributed to the two-fermionic degrees of freedom, i.e., protons and neutrons, which is unique to atomic nuclei.

ACKNOWLEDGMENTS

The (^{3}He,t) experiment was performed at RCNP, Osaka University, under Experimental Program No. E307. The authors thank the accelerator group of RCNP for providing a high-quality ^{3}He beam. Y.F. acknowledges the discussions

with W. Gelletly (Surrey), K. Matsuyanagi (Kyoto, RIKEN), K. Muto (Tokyo Institute of Technology), and H. Toki (Osaka). Y.F. also acknowledges the support of MEXT, Japan under Grants No. 18540270, No. 22540310, and No. 15K05104. Y.F. and B.R. are grateful for the support of the Japan-Spain collaboration program by JSPS and CSIC; A.A., E.E.A., and B.R. are thankful for the support of Spanish Ministry under Grants No. FPA2005-03993, No. FPA2008-06419-C02-01, and No. FPA2011-24553. G.S. acknowledges the support of TUBITAK, Turkey under Research Scholarship No. BIDEB 2214. J.M.D., C.J.G., R.M., G.P., and R.G.T.Z. are grateful for the support of the US NSF under Grants No. PHY-0606007 and No. PHY-0822648 (JINA). M.C., J.G., and A.K. acknowledge the support of the OTKA Foundation, Hungary, under Grant No. K106035. This work was in part supported by the RIKEN-CNS joint research project on large-scale nuclear-structure calculations.

[1] A. Bohr and B. R. Mottelson, *Nuclear Structure* (Benjamin, New York, 1969), Vol. 1.
[2] F. Osterfeld, Rev. Mod. Phys. **64**, 491 (1992), and references therein.
[3] B. Rubio and W. Gelletly, Lect. Notes Phys. **764**, 99 (2009).
[4] Y. Fujita, B. Rubio, and W. Gelletly, Prog. Part. Nucl. Phys. **66**, 549 (2011), and references therein.
[5] M. N. Harakeh and A. van der Woude, *Giant Resonances*, Oxford Studies in Nuclear Physics (Oxford University Press, Oxford, 2001), Vol. 24, and references therein.
[6] R. A. Broglia and V. Zelevinsky (eds.), *Fifty Years of Nuclear BCS, Pairing in Finite Systems* (World Scientific, Singapore, 2013).
[7] Y. Fujita *et al.*, Phys. Rev. Lett. **112**, 112502 (2014).
[8] C. L. Bai, H. Sagawa, G. Colò, Y. Fujita, H. Q. Zhang, X. Z. Zhang, and F. R. Xu, Phys. Rev. C **90**, 054335 (2014).
[9] K. Langanke and G. Martínez-Pinedo, Rev. Mod. Phys. **75**, 819 (2003).
[10] J. Rapaport and E. Sugarbaker, Annu. Rev. Nucl. Part. Sci. **44**, 109 (1994).
[11] C. Gaarde, Nucl. Phys. A **396**, 127c (1983).
[12] T. N. Taddeucci, C. A. Goulding, T. A. Carey, R. C. Byrd, C. D. Goodman, C. Gaarde, J. Larsen, D. Horen, J. Rapaport, and E. Sugarbaker, Nucl. Phys. A **469**, 125 (1987), and references therein.
[13] W. G. Love, K. Nakayama, and M. A. Franey, Phys. Rev. Lett. **59**, 1401 (1987).
[14] Y. Fujita, Y. Shimbara, I. Hamamoto, T. Adachi, G. P. A. Berg, H. Fujimura, H. Fujita, J. Görres, K. Hara, K. Hatanaka, J. Kamiya, T. Kawabata, Y. Kitamura, Y. Shimizu, M. Uchida, H. P. Yoshida, M. Yoshifuku, and M. Yosoi, Phys. Rev. C **66**, 044313 (2002).
[15] Y. Fujita, Y. Shimbara, A. F. Lisetskiy, T. Adachi, G. P. A. Berg, P. von Brentano, H. Fujimura, H. Fujita, K. Hatanaka, J. Kamiya, T. Kawabata, H. Nakada, K. Nakanishi, Y. Shimizu, M. Uchida, and M. Yosoi, Phys. Rev. C **67**, 064312 (2003).
[16] R. G. T. Zegers *et al.*, Phys. Rev. C **74**, 024309 (2006).
[17] Y. Fujita, H. Akimune, I. Daito, H. Fujimura, M. Fujiwara, M. N. Harakeh, T. Inomata, J. Jänecke, K. Katori, A. Tamii, M. Tanaka, H. Ueno, and M. Yosoi, Phys. Rev. C **59**, 90 (1999).
[18] Y. Fujita, R. Neveling, H. Fujita, T. Adachi, N. T. Botha, K. Hatanaka, T. Kaneda, H. Matsubara, K. Nakanishi, Y. Sakemi, Y. Shimizu, F. D. Smit, A. Tamii, and M. Yosoi, Phys. Rev. C **75**, 057305 (2007).
[19] F. Molina *et al.*, Phys. Rev. C **91**, 014301 (2015).
[20] T. Adachi *et al.*, Phys. Rev. C **85**, 024308 (2012).
[21] H. Fujita *et al.*, Phys. Rev. C **75**, 034310 (2007).
[22] T. Adachi *et al.*, Phys. Rev. C **73**, 024311 (2006).
[23] Y. Fujita *et al.*, Phys. Rev. Lett. **95**, 212501 (2005).
[24] E. Ganioğlu *et al.*, Phys. Rev. C **87**, 014321 (2013).
[25] C. D. Goodman, C. C. Foster, D. E. Bainum, S. D. Bloom, C. Gaarde, J. Larsen, C. A. Goulding, D. J. Horen, T. Masterson, S. Grimes, J. Rapaport, T. N. Taddeucci, and E. Sugerbaker, Phys. Lett. B **107**, 406 (1981).
[26] See web site http://www.rcnp.osaka-u.ac.jp.
[27] T. Wakasa, K. Hatanaka, Y. Fujita, G. P. A. Berg, H. Fujimura, H. Fujita, M. Itoh, J. Kamiya, T. Kawabata, K. Nagayama, T. Noro, H. Sakaguchi, Y. Shimbara, H. Takeda, K. Tamura, H. Ueno, M. Uchida, M. Uraki, and M. Yosoi, Nucl. Instrum. Methods Phys. Res. A **482**, 79 (2002).
[28] M. Fujiwara, H. Akimune, I. Daito, H. Fujimura, Y. Fujita, K. Hatanaka, H. Ikegami, I. Katayama, K. Nagayama, N. Matsuoka, S. Morinobu, T. Noro, M. Yoshimura, H. Sakaguchi, Y. Sakemi, A. Tamii, and M. Yosoi, Nucl. Instrum. Methods Phys. Res. A **422**, 484 (1999).
[29] T. Noro *et al.*, RCNP (Osaka University), Annual Report, 1991 (unpublished), p. 177.
[30] Y. Fujita, K. Hatanaka, G. P. A. Berg, K. Hosono, N. Matsuoka, S. Morinobu, T. Noro, M. Sato, K. Tamura, and H. Ueno, Nucl. Instrum. Methods Phys. Res. B **126**, 274 (1997), and references therein.
[31] H. Fujita, G. P. A. Berg, Y. Fujita, K. Hatanaka, T. Noro, E. J. Stephenson, C. C. Foster, H. Sakaguchi, M. Itoh, T. Taki, K. Tamura, and H. Ueno, Nucl. Instrum. Methods Phys. Res. A **469**, 55 (2001).
[32] Y. Fujita *et al.*, Phys. Rev. C **88**, 014308 (2013).
[33] H. Fujita, Y. Fujita, G. P. A. Berg, A. D. Bacher, C. C. Foster, K. Hara, K. Hatanaka, T. Kawabata, T. Noro, H. Sakaguchi, Y. Shimbara, T. Shinada, E. J. Stephenson, H. Ueno, and M. Yosoi, Nucl. Instrum. Methods Phys. Res. A **484**, 17 (2002).
[34] B. Singh and J. A. Cameron, Nucl. Data Sheets **92**, 1 (2001).
[35] B. D. Anderson, M. Mostajabodda'vati, C. Lebo, R. J. McCarthy, L. Garcia, J. W. Watson, and R. Madey, Phys. Rev. C **43**, 1630 (1991).
[36] Y. Shimbara *et al.*, Phys. Rev. C **86**, 024312 (2012).
[37] Y. Ichikawa *et al.*, Phys. Rev. C **80**, 044302 (2009).
[38] L. Popescu *et al.*, Phys. Rev. C **79**, 064312 (2009).
[39] D. H. Wilkinson (ed.), *Isospin in Nuclear Physics* (North-Holland, Amsterdam, 1969).
[40] A. Bohr and B. Mottelson, *Nuclear Structure* (Benjamin, New York, 1975), Vol. 2, Chap. 6, and references therein.
[41] T. Kurtukian Nieto *et al.*, Phys. Rev. C **80**, 035502 (2009).
[42] J. C. Hardy and I. S. Towner, Phys. Rev. C **79**, 055502 (2009), and references therein.
[43] J. C. Hardy and I. S. Towner, Nucl. Phys. News **16**, 11 (2006).
[44] N. A. Smirnova and C. Volpe, Nucl. Phys. A **714**, 441 (2003).

[45] M. Karakoç *et al.*, Phys. Rev. C **89**, 064313 (2014).
[46] DW81, a DWBA computer code by J. R. Comfort (1981) used in an updated version (1986), an extended version of DWBA70 by R. Schaeffer and J. Raynal (1970).
[47] S. Y. van der Werf, S. Brandenburg, P. Grasdijk, W. A. Sterrenburg, M. N. Harakeh, M. B. Greenfield, B. A. Brown, and M. Fujiwara, Nucl. Phys. A **496**, 305 (1989).
[48] R. Schaeffer, Nucl. Phys. A **164**, 145 (1971).
[49] R. G. T. Zegers *et al.*, Phys. Rev. Lett. **90**, 202501 (2003); S. Y. van der Werf and R. G. T. Zegers (private communication).
[50] T. Yamagata, H. Utsunomiya, M. Tanaka, S. Nakayama, N. Koori, A. Tamii, Y. Fujita, K. Katori, M. Inoue, M. Fujiwara, and H. Ogata, Nucl. Phys. A **589**, 425 (1995).
[51] W. G. Love and M. A. Franey, Phys. Rev. C **24**, 1073 (1981).
[52] J. A. Cameron and B. Singh, Nucl. Data Sheets **102**, 293 (2004).
[53] M. Honma, T. Otsuka, B. A. Brown, and T. Mizusaki, Phys. Rev. C **69**, 034335 (2004).
[54] M. Honma, T. Otsuka, T. Mizusaki, M. Hjorth-Jensen, and B. A. Brown, J. Phys.: Conf. Ser. **20**, 7 (2005).
[55] A. Poves, J. Sánchez-Solano, E. Caurier, and F. Nowacki, Nucl. Phys. A **694**, 157 (2001).
[56] K. Ikeda, S. Fujii, and J. I. Fujita, Phys. Lett. **3**, 271 (1963).
[57] M. Ichimura, H. Sakai, and T. Wakasa, Prog. Part. and Nucl. Phys. **56**, 446 (2006), and references therein.
[58] K. Yako *et al.*, Phys. Rev. Lett. **103**, 012503 (2009).
[59] D. J. Mercer, G. M. Crawley, S. Danczyk, A. Galonsky, J. Wang, A. Bacher, G. P. A. Berg, A. C. Betker, W. Schmidt, and E. J. Stephenson, IUCF Sci. and Tech. Rep. 1994-1995, Indiana University (unpublished), p. 20, https://scholarworks.iu.edu/dspace/handle/2022/465.
[60] E. Lipparini and S. Stringari, Phys. Rep. **175**, 103 (1989).
[61] C. Djalali, N. Marty, M. Morlet, A. Willis, J. C. Jourdain, N. Anantaraman, G. M. Crawley, A. Galonsky, and P. Kitching, Nucl. Phys. A **388**, 1 (1982).
[62] C. Djalali, N. Marty, M. Morlet, A. Willis, J. C. Jourdain, N. Anantaraman, G. M. Crawley, A. Galonsky, and J. Duffy, Nucl. Phys. A **410**, 399 (1983); **417**, 564 (1984).
[63] A. Willis, M. Morlet, N. Marty, C. Djalali, D. Bohle, H. Diesener, A. Richter, and H. Stein, Nucl. Phys. A **499**, 367 (1989).
[64] G. P. A. Berg, C. C. Foster, E. J. Stephenson, and B. F. Davis, IUCF Sci. Tech. Rep. 1993-1994, Indiana University (unpublished), p. 106, https://scholarworks.iu.edu/dspace/handle/2022/535.
[65] W. Steffen, H.-D. Gräf, W. Gross, D. Meuer, A. Richter, E. Spamer, O. Titze, and W. Knüpfer, Phys. Lett. B **95**, 23 (1980).
[66] G. F. Bertsch and Y. Luo, Phys. Rev. C **81**, 064320 (2010).
[67] G. F. Bertsch, in *Fifty Years of Nuclear BCS, Pairing in Finite Systems*, edited by R. A. Broglia and V. Zelevinsky (World Scientific, Singapore, 2013), Chap. 3, p. 26.
[68] W. Satuła and R. Wyss, Phys. Lett. B **393**, 1 (1997).
[69] A. L. Goodman, Phys. Rev. C **60**, 014311 (1999).
[70] A. Gezerlis, G. F. Bertsch, and Y. L. Luo, Phys. Rev. Lett. **106**, 252502 (2011).
[71] K. Yoshida, Phys. Rev. C **90**, 031303(R) (2014).
[72] E. P. Wigner, Phys. Rev. **51**, 106 (1937).
[73] D. R. Tilley, C. M. Cheves, J. L. Godwin, G. M. Hale, H. M. Hofmann, J. H. Kelley, C. G. Sheu, and H. R. Weller, Nucl. Phys. A **708**, 3 (2002).
[74] D. R. Tilley, H. R. Weller, C. M. Cheves, and R. M. Chasteler, Nucl. Phys. A **595**, 1 (1995).
[75] B. D. Anderson, A. Fazely, R. J. McCarthy, P. C. Tandy, J. W. Watson, R. Madey, W. Bertozzi, T. N. Buti, J. M. Finn, J. Kelly, M. A. Kovash, B. Pugh, B. H. Wildenthal, and C. C. Foster, Phys. Rev. C **27**, 1387 (1983).
[76] J. Rapaport, C. C. Foster, C. D. Goodman, C. A. Goulding, T. N. Taddeucci, D. J. Horen, E. R. Sugarbaker, C. Gaarde, J. Larsen, J. A. Carr, F. Petrovich, and M. J. Threapleton, Phys. Rev. C **41**, 1920 (1990).
[77] K. Ikeda, T. Myo, K. Kato, and H. Toki, in *Clusters in Nuclei*, edited by C. Beck, Lecture Notes in Physics Vol. 818 (Springer, Berlin, 2010), Chap. 5, p. 165.
[78] E. Garrido, P. Sarriguren, E. Moya de Guerra, and P. Schuck, Phys. Rev. C **60**, 064312 (1999).
[79] E. Garrido, P. Sarriguren, E. Moya de Guerra, U. Lombardo, P. Schuck, and H. J. Schulze, Phys. Rev. C **63**, 037304 (2001).
[80] E.-W. Grewe *et al.*, Phys. Rev. C **76**, 054307 (2007).
[81] B. L. Berman and S. C. Fultz, Rev. Mod. Phys. **47**, 713 (1975).